ORIGINAL CONTRIBUTION

CrossMark

Synthesis of large pore sized ordered mesoporous carbons using triconstituent self-assembly strategy under different acidic conditions and ratios of carbon precursor to structure directing agent

Silver Güneş[1] · Çiğdem Güldür[2]

Abstract

This study was aimed at the synthesis of ordered mesoporous carbons with large pores. A triconstituent self-assembly strategy was employed, where resorcinol and formaldehyde were used as carbon source, tetraethyl orthosilicate was used as silica source, and triblock copolymer Pluronic F127 was used as structure directing agent. The effects of hydrochloric acid (HCl) concentration on the composite yield and the textural properties of carbons were investigated. The composite yield was seen to increase until a HCl concentration of 0.66 M. The effect of carbon source (resorcinol-formaldehyde (RF)) to Pluronic F127 ratio (RF/F127) was also investigated. The pore sizes slightly varied around 6 nm at low RF/F127 ratios, while the RF/127 = 2 ratio gave a 8.1-nm pore size and 711-m^2/g surface area. The resultant carbons are promising for use in areas such as fuel cells, where diffusion limitations affect the performance.

Keywords Ordered mesoporous carbon · Self-assembly · Triblock copolymer · Composite

Introduction

Polymer electrolyte membrane (PEM) fuel cells are widely considered to be one of the most promising alternative energy technologies. As in many other engineering applications involving precious metal catalysts, carbons are employed at fuel cell electrodes to support platinum [1, 2]. The properties of the catalyst support affect the mass transfer of the reactant gases and the accessibility of catalytic sites [3]. In general, it is desirable for a support to have an ordered structure with large pores to provide an effective mass transfer and enable an even distribution of catalyst particles during metal loading. Although carbon blacks are economical and easily obtainable materials, they have shortcomings due to their disordered structures. They have a significant portion of micropores which are not fully accessible and known to be poorly interconnected [3]. Today, the research studies are focused on the development of new support materials with more advanced properties. Ordered mesoporous carbons (OMCs) constitute a relatively new family of materials with many potential applications, one of which is the PEM fuel cells [4–11].

The early methods for the OMC synthesis were based on the use of mesoporous silica templates such as MCM-41 and SBA-15 [12–14]. These template-based methods require the separate synthesis of a silica template which is then infiltrated with a carbon source and finally removed by etching after carbonization. Although the template method yields well-ordered structures, the pore size of these carbons is typically less than 5 nm. Since the catalyst particles often have comparable sizes, these OMCs are disadvantageous for metal loading and impractical for PEM fuel cell applications [13]. The small pore size is disadvantageous for gas diffusion as well. Moreover, the template-based methods do not allow an efficient control over the pore size and texture as the properties of the final product are limited by the properties of template.

The more recently developed direct synthesis methods provide a more flexible route, in which the pores can be tailored by adjusting various synthesis parameters. This technique can either be described as a "soft-template" process (colloidal template) [15], or an organic (sometimes organic-inorganic) self-assembly [16, 17]. The direct synthesis is analogous to the

✉ Silver Güneş
silver@gazi.edu.tr

1 Institute of Natural and Applied Sciences, Gazi University, Beşevler, 06500 Ankara, Turkey

2 Faculty of Engineering, Chemical Engineering Department, Gazi University, Maltepe, 06570 Ankara, Turkey

Springer

synthesis of mesoporous silicas, in that the OMC is synthesized directly from the polymerization of a carbon source in the presence of a structure directing agent. By this method, larger pores can be obtained which both facilitate the mass transfer and provide a better metal loading. This procedure is also more cost-effective and involves fewer steps than the template-based methods.

Direct synthesis was pioneered by Raghuveer et al. who used cetyl trimethyl ammonium bromide (CTAB) as surfactant and aniline as the carbon source. This method produced large pores (10–40 nm) at certain CTAB/aniline ratios, but the resultant materials had poorly ordered structures [15, 18]. Since then, direct synthesis method was adopted by many researchers due to its versatility, as it allowed the use of wide varieties of surfactants and carbon sources. Triblock copolymers such as Pluronic F127 proved to be very effective as surface directing agents [16, 19–21]. Typically, phenol or phloroglucinol would be used as carbon source. The resorcinol and formaldehyde combination as a carbon source has been increasingly popular in recent years [22, 23], especially in fuel cell-related studies [24, 25]. The relative ease of obtaining these materials and a multitude of synthesis parameters led to the better control of pore size. One of the most extensively studied parameters was the concentration of the main constituents, often relative to each other such as the molar (or mass) ratio of the carbon source to the structure directing agent [26–28]. Studies show that the adjustment of the species concentrations can lead to different micelle formations ranging from rod shape to spherical and give OMCs with different structures. It was reported that higher F127/RF ratios are more likely to give 3D structures [26]. However the relationship between the carbon source concentration and the resultant carbon structure is complex and has yet to be elucidated.

Other studied parameters include the ethanol to water ratio [29], temperature of heat treatment [30], and reaction time of polymerization [31]. The acidity is well known to affect the cross-linking behavior in polymerization of silicates, but its effect in the synthesis of mesoporous carbons is rarely studied. It was reported that highly acidic concentrations prevent the later shrinkage of the polymer texture under heat treatment, leading to larger pores [32]. In another study, ultra-large pores up to 19.2 nm were created by using phloroglucinol and formaldehyde under highly acidic conditions in the expense of an ordered structure [33]. When taken together with other parameters affecting the structure, the effect of acid concentration is not sufficiently studied in literature.

Incorporation of silicates into the soft template synthesis is an alternative approach aimed to increase the pore size [34–40]. It was shown that tetraethyl orthosilicate (TEOS) can easily participate in the self-assembly of organic species to form silica/polymer composites [41, 42]. The main advantage of silica is that it forms a rigid framework within the silica/polymer composite and prevents the structural

shrinkage during the heat treatment, leading to larger pores [43]. Another advantage of using silicates is the creation of micropores after the etching process, which provides pore connections and a three-dimensional mass transfer medium. Silicates also can be bound favorably to the micelles by hydrogen bonds and increase the pore size [44]. Although the triconstituent system often leads to less ordered structures, the large pores and 3D framework is advantageous for fuel cell applications.

Here in this study, we report on the synthesis of large pore sized ordered mesoporous carbons using a triconstituent direct synthesis under different acid concentrations and precursor ratios. The synthesis procedure consists of the self-assembly of polymer/silica composite around structure directing agent, Pluronic F127. Resorcinol and formaldehyde were used as carbon source for the polymerization, while silica was incorporated in the form of TEOS. The effects of acidity on the pore texture and composite yield were investigated. The effect of mass ratio of RF/F127 was also taken into consideration. The resultant composites and carbons were characterized by thermogravimetric analysis, nitrogen adsorption, X-ray powder diffraction, and transmission electron microscopy. By tuning the synthesis conditions, large pore sized carbons suitable for fuel cell applications were developed.

Materials and methods

Materials

Amphiphilic triblock copolymer Pluronic F127 ($EO_{106}PO_{70}EO_{106}$, EO (ethylene oxide), PO (propylene oxide), $M_w = 12{,}600$ g/mol) was purchased from Sigma-Aldrich. Resorcinol (99%) and formaldehyde (37% *w/w*) as carbon sources were obtained from Merck and Sigma-Aldrich, respectively. TEOS (98%) was obtained from Sigma-Aldrich and used as the silica source. Hydrochloric acid (HCl, 37% *w/w*) was used as polymerization catalyst. Ethanol and deionized water were used as the solvent.

Synthesis of OMCs

OMCs were prepared by a triconstituent self-assembly method where Pluronic F127 was used as structure directing agent, resorcinol and formaldehyde were used as carbon source, and TEOS was used as the silica source. For a typical synthesis (RF/F127 = 2/1), 1.25 g resorcinol and 1.25 g Pluronic F127were dissolved in 50 ml water-ethanol (2:3 *v/v*) solution and stirred for 15 min. Afterwards, HCl was added as polymerization catalyst and the solution was stirred for another 15 min. Then, 1.25 g formaldehyde and 1.87 g TEOS were added and the solution was kept under vigorous stirring for 30 min. The mass ratio of carbon source (resorcinol and

formaldehyde) to Pluronic F127 was set between 1:4 and 4:1 to study the effect of the RF/F127 ratio, and the HCl concentration was varied between 0.22 and 0.88 M to study the effect of acid concentration. The solution was kept still in room temperature for 4 days to ensure that the polymerization reaction is complete. At the end of this period, the solution separated into two phases; a bottom composite-rich phase and an upper ethanol-rich phase. The ethanol-rich phase was discarded while the composite phase was transferred to a Petri dish and dried in an oven at 110 °C. Then, the composite was grinded and carbonized under controlled argon atmosphere at 180 °C for 1 h, 400 °C for 4 h, and 700 °C for 1 h using a tube furnace (Protherm, ASP series). Finally, the carbonized material was etched by 15% HF to remove the silica in the composite structure.

Characterization

The composites and carbons were physically characterized by thermogravimetric analysis (TGA), nitrogen physisorption, X-ray powder diffraction (XRD), and transmission electron microscope (TEM). Temperature-programmed TGA was applied to the composite samples taken prior to the carbonization stage to see the physicochemical changes in the samples during the carbonization. Measurements were conducted between 30 and 850 °C using a Setaram LABSYS thermogravimeter. Nitrogen physisorption analysis was performed in order to investigate the surface areas, pore size distributions, and pore volumes of the carbons using an Autosorb-6B model Quantachrome sorptometer. Samples were preheated at 110 °C before the analysis. Specific surface areas were calculated by the BET (Brunauer-Emmett-Teller) method. The pore size distributions and pore volumes were calculated from the adsorption branches of isotherms using the BJH (Barrett-Joyner-Halenda) method.

The ordered mesostructure of the carbons were investigated by XRD using a Rigaku Ultima IV diffractometer with a 40-kV excitation potential and Cu Kα radiation (λ = 1.5406 Å). Measurements were performed between 2θ = 0.2–30° with a scan rate of 0.02°/min. Interplanar spacings were calculated by the Scherrer equation. Pore structures of the samples were investigated by TEM analysis using a 200 kV Jem Jeol 2100F model HRTEM microscope.

Results and discussions

Effect of the HCl concentration

To study the effect of HCl concentration, samples were prepared at different HCl concentrations (between 0.22 and 0.88 M) and then assigned as OMC-H22, OMC-H44, OMC-H66, and OMC-H88. The dry masses of the polymer/silica composites were measured before the carbonization process. Figure 1 shows that the total composite mass increases with the acid concentration until it reaches a steady value at around 0.66 M. It should be noted that the total composite mass consists of polymer, silica, triblock copolymer, unreacted resorcinol and formaldehyde, and possibly some water and ethanol, so the reaction yield of polymerization can only be assessed after TGA analysis. Nevertheless, Fig. 1 shows that the composite mass varies with the acid concentration due to the latter's effect on the polymerization reaction mechanism.

TGA analysis was performed to investigate the composition and the physicochemical changes during the carbonization stage. The change in mass seems to follow similar trends in all the samples, except some slight differences under 380 °C (Fig. 2). This shows that although the HCl concentration affects the total composite mass, it does not have a strong effect on the composition due the phase equilibrium in the synthesis solution.

Over 850 °C temperature, the remaining mass constitutes about 25% of the initial composite mass. The sharpest decrease in the mass occurs between 390 and 410 °C due to the decomposition of triblock copolymer Pluronic F127. A loss of about 15% occurs up to that temperature, mainly because of the evaporation of water, ethanol, and the unreacted resorcinol and formaldehyde. This shows that the polymer-rich composite phase contains 60% triblock copolymer by mass at the beginning. This is a reasonable value considering that the pores are filled with the micelles formed by Pluronic F127.

The slight mass changes between 50 and 100 °C are mostly due to the evaporation of water and shows that the polymeric phases still contain some 3–4% water in the structure even after the drying process. It is seen that the mass changes slow down after 410 °C and become negligible over 700 °C. In previous works, pure Pluronic F127 was reported to be decomposed by a 97% ratio at 410 °C [27]. The 10–15% mass change still occurring over 410 °C may be attributed to the side products and other defects in the polymer chain after the condensation reaction between resorcinol and formaldehyde.
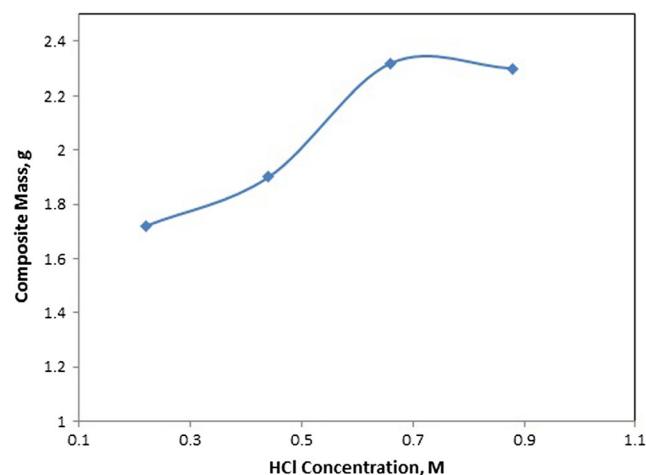

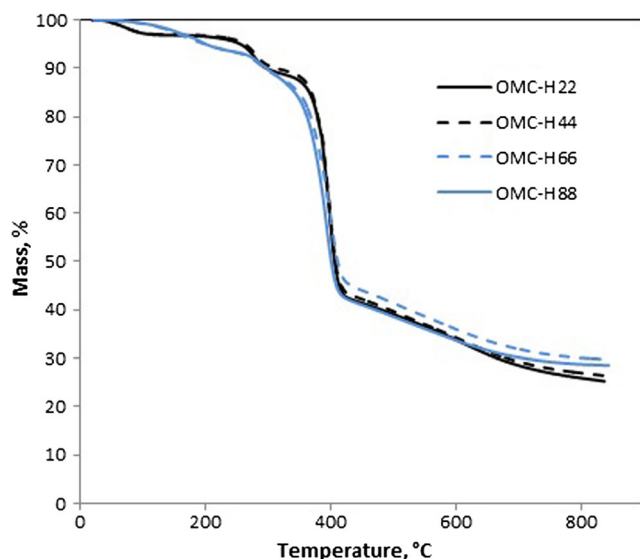**Fig. 1** Variation of the composite mass with the HCl concentration

Fig. 2 TGA analysis of composite samples prepared at different HCl concentrations

By assuming a R/F stoichiometric ratio of 1:2 for the polymerization reaction, the mass yields were calculated to be between 22 and 30% for the OMC samples (Table 1). Since the compositions of the samples do not vary with the acid concentration, it can be concluded that the variation of the polymerization yield with the acid concentration follows the same trend in Fig. 1 and the reaction is completed at around 0.66 M.

Nitrogen physisorption analysis was carried out to investigate the pore structures of the OMC samples prepared at different acid concentrations. Adsorption/desorption isotherms show that all samples have predominantly mesoporous structures, as the capillary condensation steps are clearly evident in the middle relative pressure values (Fig. 3a). The OMC-H44 carbon is distinguished from the others as the capillary condensation occurs at higher relative pressures, suggesting a larger pore size. For the other HCl concentrations, the capillary condensations occur nearly at the same relative pressure range indicating that their pore sizes are close to each other. The lowest HCl concentration gives a smaller surface area, which is evident from the amount of nitrogen adsorbed throughout the cycle. It is noteworthy that acid concentrations of 0.66 and 0.88 M give nearly overlapping isotherms and show

that the effect of the acid concentration is less pronounced over 0.66 M.

All the isotherms exhibit type IV behavior with H1 type hysteresis loops, signifying a uniform pore size distribution. This is evident in the pore size distribution where all samples give well-defined peaks typical of unimodal pore architectures (Fig. 3b). The OMC-H44 sample has a broader distribution and a larger mean pore size. The pore size distributions of the carbons prepared at 0.66 and 0.88 M are very similar and indicative of smaller sized but well ordered pores. Surface areas, mean pore diameters, and pore volumes of the carbons prepared at different acid concentrations are listed in Table 2.

It is evident that the HCl concentration not only affects the reaction mass yield but also the final morphology through the polymerization mechanism. However, the influence of acid concentration is less significant after 0.66 M at which point the reaction is completed. The highest surface area was measured from the OMC-H44 carbon as 711 m^2/g, slightly greater than OMC-H66 and OMC-H88. It is interesting that the same carbon has the largest pore size also, with 8.1 nm. This can be explained by a combination of an exceptionally high total pore volume of 0.75 cm^3/g, resulting from thinner pore walls due to a not fully competed polymerization, and a slightly greater micropore volume which is the main contributor to the surface area. In the case of OMC-H22 with the lowest HCl concentration, the small surface area and the exceptionally small micropore volume suggest that a lower degree of polymerization leads to a simpler, unimodal pore structure. Thus, the increase of the HCl concentration seems to promote the formation of micropores by branching of the polymer chain. The significant volumes of micropores in the samples can also be attributed to the inclusion of TEOS. According to the literature, micropores created by the etching of TEOS may have an enhancing effect on the mass transfer by serving as connections between the mesopores [44].

Wide-angle XRD spectra showed broad peaks at $2\Theta = 23°$ due to (002) diffraction of the amorphous carbon crystal structure. Low-angle XRD patterns of the carbons are shown in Fig. 4. Intense peaks in the region $2\Theta = 0.4$–$0.45°$ for all carbons indicate an ordered mesostructure. There are also less intense reflections at 0.74° for H66 and H88, 0.84° for H22, and a weaker shoulder for H44. These secondary reflections may be either due to the long-range (110) mesostructures or due to the presence of uniform micropore textures. The OMC-

Table 1 Polymerization mass yields of composites prepared at different HCl concentrations (OMC-H22; 0.22 M HCl, OMC-H44; 0.44 M HCl, OMC-H66; 0.66 M HCl, OMC-H88; 0.88 M HCl)

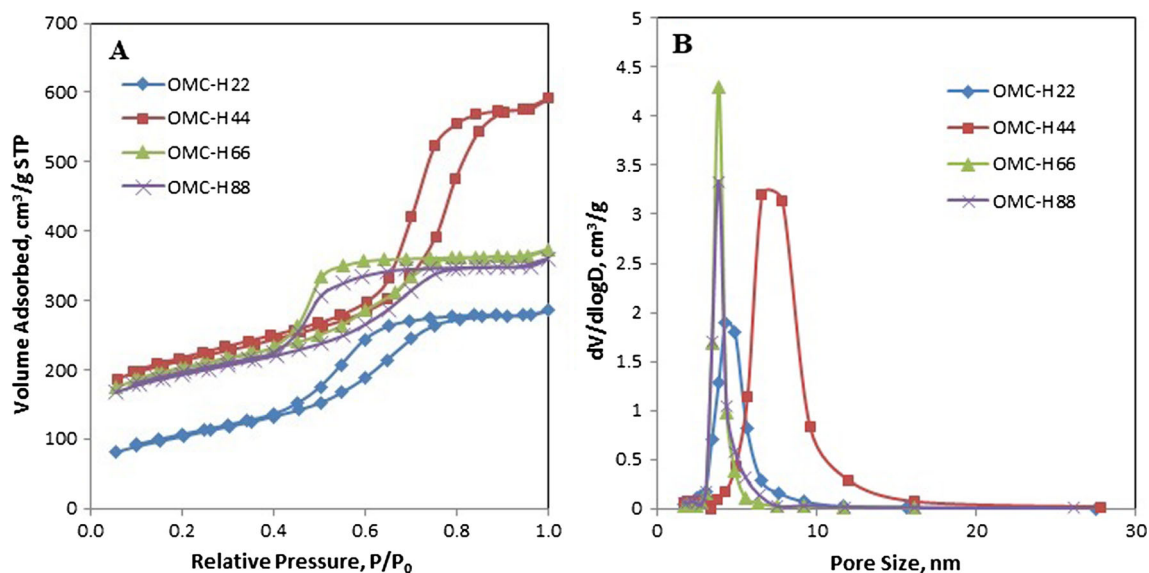| Yield	OMC-H22	OMC-H44	OMC-H66	OMC-H88
Total composite mass (g)	1.72	1.90	2.32	2.30
Polymer/silica mass (g)	0.43	0.475	0.58	0.575
Mass yield (%)	22.4	24.7	30.2	29.9

Fig. 3 **a** BET isotherms of OMC-H22, OMC-H44, OMC-H66, and OMC-H88 carbons prepared at different acid concentrations. **b** Pore size distributions of OMC-H22, OMC-H44, OMC-H66, and OMC-H88 carbons prepared at different acid concentrations

H44 carbon has the weakest of these secondary peaks, probably due to a convergence of the micropore reflections with the main mesopore peak. A less intense main peak in OMC-H44 carbon confirms a lower degree of order but a slightly wider pore size distribution. The position of the peak is also at a smaller angle (0.42°) indicating a wider d-spacing.

The patterns suggest that these carbons have three-dimensional wormhole structures. Bragg equation gives an approximate d-spacing of 10.5 nm for OMC-H44 (for the peak at $2\Theta = 0.42°$) and 9.8 nm for OMC-H66 and OMC-H88 (for the peaks at $2\Theta = 0.45°$). Considering the fact that the wall thickness is also contributing to the plane spacing, these values are consistent with the results found with the nitrogen adsorption analysis.

Effect of the carbon source to surfactant (RF/ F127) ratio

Among the carbons prepared at different acid concentrations, the largest pore size was obtained from the OMC-H44 sample; therefore, the HCl concentration was kept constant at 0.44 M in the subsequent synthesis. Carbons were synthesized at different RF/F127 ratios varying between 0.25 and 4 (RF = C,

F127 = P; OMC-H44-C1P4, OMC-H44-C1P2, OMC-H44-C1P1, OMC-H44-C2P1, OMC-H44-C4P1). OMC-H44 and OMC-H44-C2P1 are identical since the former was already synthesized in RF/F127 = 2 ratio. The changes in the physical properties were apparent after the phase separation, as the RF/F127:0.25 ratio gave yellow colored composite phase while the RF/F127:4 ratio produced red colored composite phase. Figure 5a shows the nitrogen adsorption-desorption isotherms of different carbon samples synthesized in varying RF/F127 ratios.

The OMC-H44-C4P1 carbon with the highest RF/F127 ratio is seen to have a distinguished isotherm for which adsorption and desorption branches do not overlap at the end of the cycle. The adsorbed nitrogen volume is also significantly low for this sample. This indicates a microporous structure with a smaller surface area compared to the other carbons. The separated branches of adsorption and desorption are possibly due to the partial blockage of pores after the adsorption and hindering the desorption. This situation is typical for microporous polymers and shows that the sample has an elastic structure. In any case, it appears clearly that the OMC-H44-C4P1 does not possess favorable features regarding fuel cell applications. Except for the aforementioned carbon, all other

Table 2 Textural properties of carbons prepared at different acid concentrations

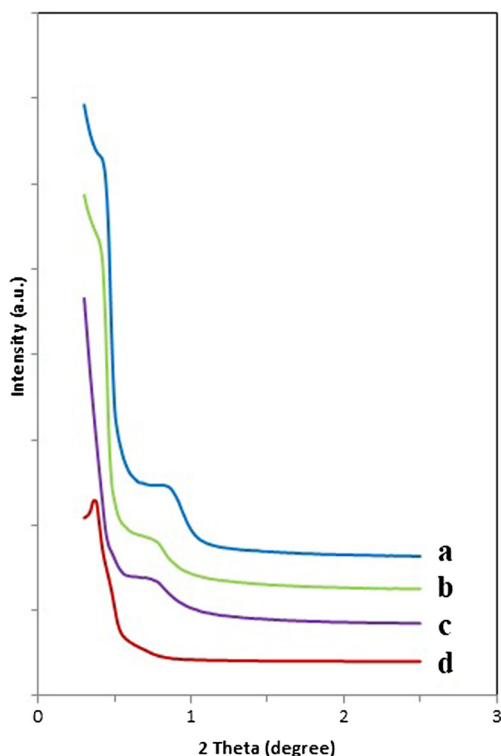| Carbon sample	S_T (m^2/g)	D_{ads} (nm)	D_{des} (nm)	D_{avg} (nm)	V_T (cm^3/g)	V_m (cm^3/g)
OMC-H22	365	5.6	4.3	5.0	0.42	0.18
OMC-H44	711	9.5	6.6	8.1	0.75	0.35
OMC-H66	675	4.9	3.9	4.4	0.45	0.33
OMC-H88	669	5.6	3.9	4.8	0.41	0.32

Fig. 4 XRD patterns of OMCs prepared at different HCl concentrations, (**a**) OMC-H22, (**b**) OMC-H66, (**c**) OMC-H88, and (**d**) OMC-H44

samples exhibit type IV adsorption-desorption isotherms showing predominantly mesoporous structures. Isotherms for RF/F127 ratios of 0.5 and 1 are almost identical, suggesting that the C/P ratio has little influence on the structure in this range. On the other hand, carbons with RF/127 = 0.25 and 2 show sharper pore condensation transitions, indicative of greater mesopore volumes. As seen in Fig. 5b, all carbons except OMC-H44-C4P1 have narrow pore size distributions

with their peaks centering around 5–6 nm for RF/F127 ratios from 0.25 to 1 and 8 nm for RF/F127 = 2. OMC-H44-C1P4 features a distinctly narrower pore size distribution and a more uniform pore structure. However, OMC-H44-C2P1 has a larger mean pore size which is more advantageous for fuel cell applications. Except for OMC-H44-C4P1, the surface areas are between 689 and 714 m^2/g and do not differ significantly. Surface areas, pore sizes, and pore volumes are summarized in Table 3.

Aside from OMC-H44-C2P1 with the largest pore size, most of the samples have mean pore sizes near 6 nm which may be deemed adequate for fuel cell applications. The pore volumes also differ with the RF/F127 ratio. The large pore volumes of OMC-H44-C1P4 and OMC-H44-C2P1 are thought to be due to the decreased wall thickness. In general, the smaller RF/F127 ratios produced well-ordered carbons with narrower pore size distributions and smaller pores. At higher RF/F127 ratios, the pore size is larger but the structure is less ordered. This may be explained by the change in the packing parameter, which can be defined as the ratio of the carbonaceous phase to the surfactant phase within a unit cell. It has been reported that higher carbon source concentrations cause the micelles attached to the carbon framework to swell and lead to larger pores [27]. It can be concluded that higher RF/F127 ratios lead to less ordered structures and values over RF/F127 = 4 give totally disordered and microporous carbons. Therefore, besides affecting the polymer wall thickness and swelling of micelles, the carbon source concentration also affects the formation and size of the micelles at higher concentrations. Similarly, Long et al. reported that over a RF/F127 ratio of 5, disordered structures are formed, while the most ordered structure is formed at a RF/F127 ratio of 2.5 and RF/F127 ratios between 2 and 2.5 give three-dimensional body centered cubic structures [31].
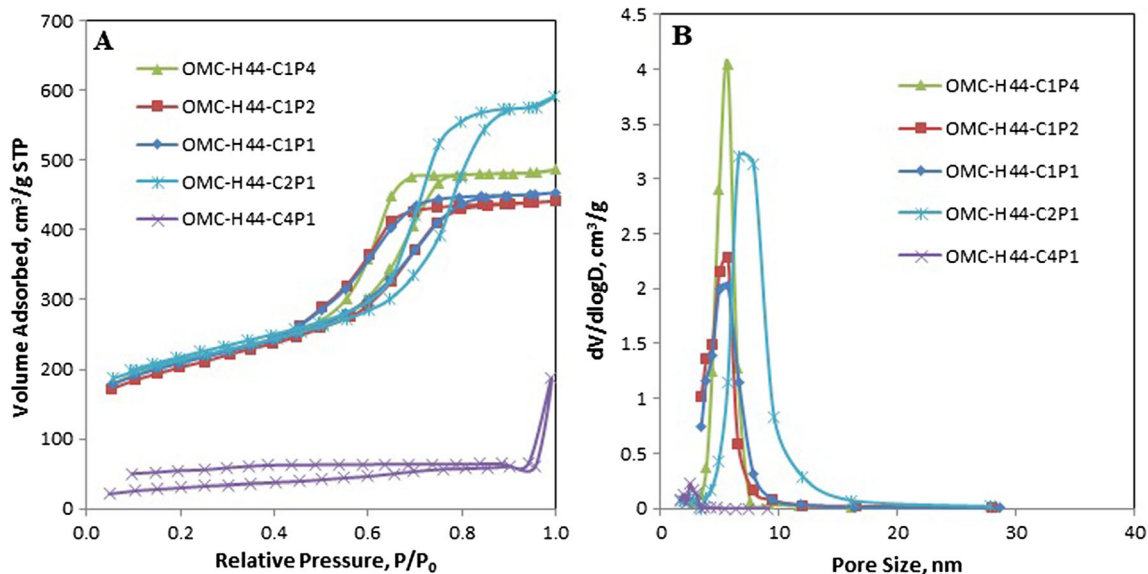

Fig. 5 **a** Nitrogen adsorption isotherms of the OMC samples synthesized in different RF/F127 ratios (OMC-H44-C1P4, OMC-H44-C1P2, OMC-H44-C1P1, OMC-H44-C2P1, OMC-H44-C4P1). **b** Pore size distributions of the OMC samples synthesized in different RF/F127 ratios

**Table 3** Textural properties of carbons prepared at different RF/ F127 ratios

RF/F127 ratio	S_{BET} (m^2/g)	D_{ads} (nm)	D_{des} (nm)	D_{avg} (nm)	V_T (cm^3/g)	V_m (cm^3/g)
1:4	714	6.5	5.6	6.1	0.62	0.32
1:2	689	6.6	4.9	5.8	0.56	0.30
1:1	704	6.5	4.9	5.7	0.56	0.31
2:1	711	9.5	6.6	8.1	0.75	0.35
4:1	110	1.4	2.5	2.0	0.29	/

TEM analysis

Physical characterization studies showed that the OMC-H44-C2P1, OMC-H44-C1P2, and OMC-H44-C1P4 carbons have comparatively large mean pore sizes and uniform mesostructures. TEM images of the corresponding samples are shown in Fig. 6. All samples exhibit three-dimensional wormhole-like structures which can be defined by the Ia3d symmetry group. Although the regularity of the mesopores is not of a high level, the interconnected structure is advantageous for fuel cell applications, as three-dimensional framework in porous carbons is known to facilitate the mass

Fig. 6 TEM images of **a**, **b** OMCH44-C2P1, **c**, **d** OMC-H44-C1P4, and **e**, **f** OMC-H44-C1P2 carbons
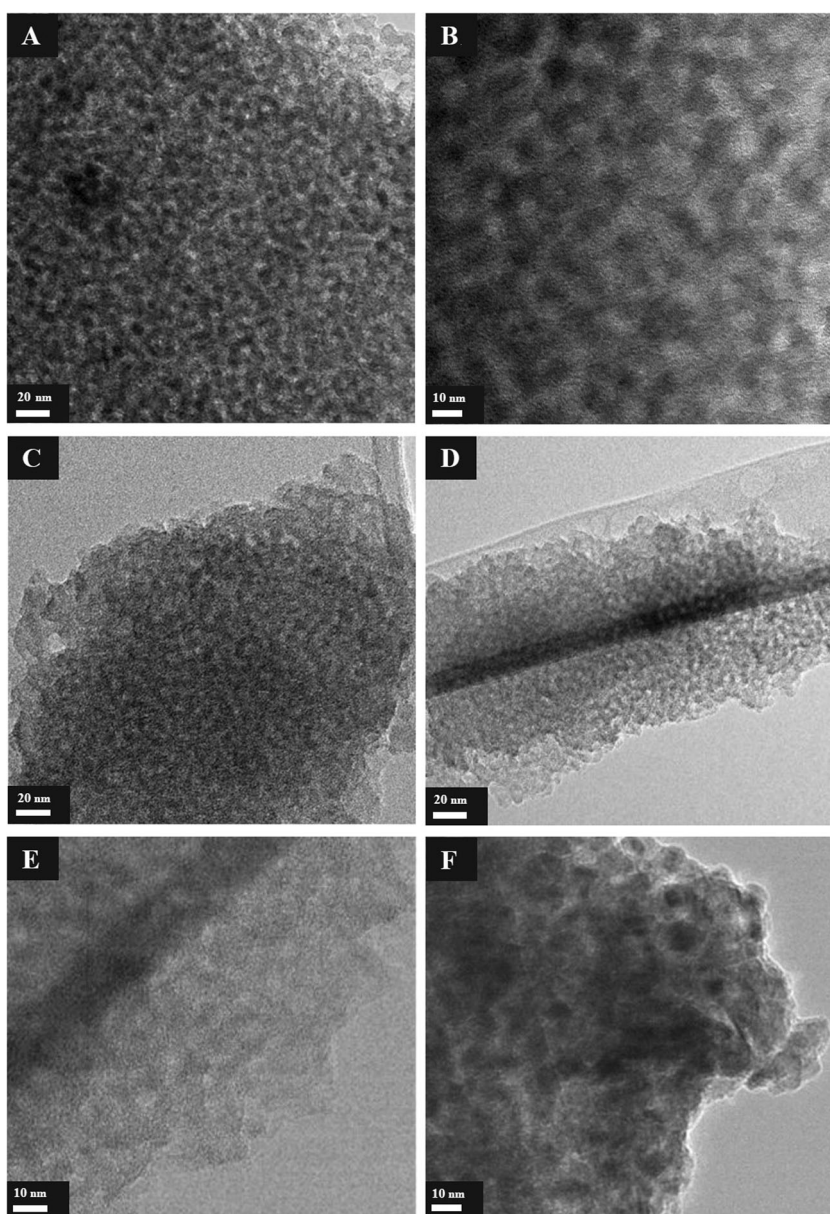
transport [45]. From the bright and dark regions, the pore size of the OMC-H44-C2P1 carbon can be roughly measured to be around 10 nm. This is consistent with the findings of the nitrogen adsorption and XRD analysis and even shows that the size based on the desorption branch (9.5 nm) has better proximity to the one observed from TEM images.

Conclusions

Employing a triconstituent self-assembly strategy and by tuning the HCl concentration and RF/F127 ratio, a carbon with a pore diameter of 8.1 nm and a surface area of 711 m^2/g was successfully synthesized. The composite yield was seen to increase with HCl concentration until the completion of the polymerization reaction at around 0.66 M. The textural properties were not affected by acid concentration after 0.66 M in accordance with the completion of polymerization. The largest pore size (8.1 nm) was obtained at an acid concentration of 0.44 M and a RF/F127 ratio of 2. Smaller RF/F127 ratios also gave pore sizes near 6 nm. These carbons exhibited 3D wormhole-like structures, which is advantageous for mass transport. It can be concluded that the aforementioned OMC-H22-C2P1 carbon can be used as a support material in fuel cells and other applications where larger pore sizes are needed.

Compliance with ethical standards

Conflict of interest The authors declare that they have no conflict of interest.

References

1. Auer E, Freund A, Pietsch J, Tacke T (1998) Carbons as supports for industrial precious metal catalysts. Appl Catal A 173:259–271
2. Litster S, McLean G (2004) PEM fuel cell electrodes. J Power Sources 130:61–76
3. Antolini E (2009) Carbon supports for low-temperature fuel cell catalysts. Appl Catal B 88:1–24
4. Chang H, Joo S, Pak C (2007) Synthesis and characterization of mesoporous carbon for fuel cells. J Mater Chem 17:3078–3088
5. Sahu A, Sridhar P, Pitchumani S (2009) Mesoporous carbon for fuel cell electrodes. J Indian InstSci 89:437–445
6. Sun Z, Zhang X, Liang Y, Tong H, Xue R, Yang SD, Li H (2009) Ordered mesoporous carbons (OMCs) as supports of electrocatalysts for direct methanol fuel cells (DMFCs): effect of the pore characteristics of OMCs on DMFCs. JElectroanal Chem 633:1–6
7. Calvillo L, Gangeri M, Perathoner S, Centi G, Moliner R, Lazaro M (2011) Synthesis and performance of platinum supported on ordered mesoporous carbons as catalysts for PEM fuel cells: effect

8. Hsueh Y, Yu C, Lee K, Tseng C, Su B, Wu S, Weng L (2013) Ordered porous carbon as the catalyst support for proton exchange membrane fuel cells. Int J Hydrog Energy 38:10998–11003
9. Viva F, Bruno M, Francheschini E, Thomas Y, Sanchez G, Solorza-Feria O, Corti H (2014) Mesoporous carbon as Pt support for PEM fuel cell. Int J Hydrog Energy 39:8821–8826
10. Stojmenovic M, Momcilovic M, Gavrilov N, Pasti IA, Mentus S, Jokic B, Babic B (2015) Incorporation of Pt, Ru and Pt-Ru nanoparticles into ordered mesoporous carbons for efficient oxygen reduction reaction in alkaline media. Electrochim Acta 153:130–139
11. Hung C, Liou Z, Veerakumar P, Wu P, Liu T, Liu S (2016) Ordered mesoporous carbon supported bifunctional PtM (M = Ru, Fe, Mo) electrocatalysts for a fuel cell anode. Chin J Catal 37:43–53
12. Ryoo R, Joo S, Jun S (1999) Synthesis of highly ordered carbon molecular sieves via templatemediated structural transformation. J Phys Chem B 103:7743–7746
13. Jun S, Joo SH, Ryoo R, Kruk M, Jaroniec M, Liu Z, Ohsuna T, Terasaki O (2000) Synthesis of new, nanoporous carbon with hexagonally ordered mesostructure. J Am Chem Soc 122:10712–10713
14. Stein A (2003) Advances in microporous and mesoporous solids—highlights of recent progress. Adv Mater 15:763–775
15. Raghuveer V, Manthiram A (2005) Mesoporous carbons with controlled porosity as an electrocatalytic support for methanol oxidation. J Electrochem Soc 152:1504–1510
16. Liang C, Dai S (2006) Synthesis of mesoporous carbon materials via enhanced hydrogen-bonding interaction. J Am Chem Soc 128:5316–5317
17. Tanaka S, Nishiyama N, Egashira Y, Ueyama K (2005) Synthesis of ordered mesoporous carbons with channel structure from an organic-organic nanocomposite. Chem Commun 16:2125–2127
18. Raghuveer V, Manthiram A (2004) Mesoporous carbon with larger pore diameter as an electrocatalyst support for methanol oxidation. Electrochem SolidState Lett 7:336–339
19. Meng Y, Gu D, Zhang F, Shi Y, Cheng L, Feng D, Wu Z, Chen Z, Wan Y, Stein A, Zhao D (2006) A family of highly ordered mesoporous polymer resin and carbon structures from organic–organic self-assembly. Chem Mater 18:4447–4464
20. Xie M, Dong H, Zhang D, Guo X, Ding W (2011) Simple synthesis of highly ordered mesoporous carbon by self-assembly of phenolformaldehyde and block copolymers under designed aqueous basic/acidic conditions. Carbon 49:2459–2464
21. Song L, Wang T, Xue H, Fan X, He J (2016) In-situ preparation of Pd incorporated ordered mesoporous carbon as efficient electrocatalyst for oxygen reduction reaction. Electrochim Acta 191:355–363
22. Jin J, Tanaka S, Egashira Y, Nishiyama N (2010) KOH activation of ordered mesoporous carbons prepared by a soft-templating method and their enhanced electrochemical properties. Carbon 48:1985–1989
23. Xu J, Wang A, Zhang T (2012) A two-step synthesis of ordered mesoporous resorcinol-formaldehyde polymer and carbon. Carbon 50:1807–1816
24. Hayashi A, Notsu H, Kimijima K, Miyamoto J, Yagi I (2008) Preparation of Pt/mesoporous carbon (MC) electrode catalyst and its reactivity toward oxygen reduction. Electrochim Acta 53:6117–6125
25. Ramoz-Sanchez G, Bruno M, Thomas Y, Corti H, Solorza-Feria O (2012) Mesoporous carbon supported nanoparticulated PdNi$_2$: a methanol tolerant oxygen reduction electrocatalyst. Int J Hydrog Energy 37:31–40
26. Jin J, Mitome T, Egashira Y (2011) Phase control of ordered mesoporous carbon synthesized by a soft-templating method. Colloids Surf A Physicochem Eng Asp 384:58–61

27. Li M, Xue J (2012) Ordered mesoporous carbon nanoparticles with well-controlled morphologies from sphere to rod via a soft-template route. J Colloid Interface Sci 377:169–175

28. Nishiyama N, Tanaka S (2011) Synthesis of ordered mesoporous carbon by a soft-templating method. Carbon 49:3392–3393

29. Tanaka S, Doi A, Nakatani N, Katayama Y, Miyake Y (2009) Synthesis of ordered mesoporous carbon films, powder, and fibers by direct triblock-copolymer templating method using an ethanol/water system. Carbon 47:2688–2698

30. Leonard A, Gommes C, Piedboeuf M, Pirard J, Job N (2014) Rapid aqueous synthesis of ordered mesoporous carbons: investigation of synthesis variables and application as anode materials for Li-ion batteries. Microporous Mesoporous Mater 195:92–101

31. Long D, Quiao W, Zhan L, Liang X, Ling L (2009) Effect of template and precursor chemistry on pore architectures of triblock copolymer templated mesoporous carbons. Microporous Mesoporous Mater 121:58–66

32. Wang X, Liang C, Dai S (2008) Facile synthesis of ordered mesoporous carbons with high thermal stability by self-assembly of resorcinol−formaldehyde and block copolymers under highly acidic conditions. Langmuir 24:7500–7505

33. Liu L, Wang F, Shao G, Ma T, Yuan Z (2010) Synthesis of ultra-large mesoporous carbons from triblock copolymers and phloroglucinol/formaldehyde polymer. Carbon 48:2660–2664

34. Kawashima D, Aihara T, Kobayashi Y, Kyotani T, Tomita A (2000) Preparation of mesoporous carbon from organic polymer/silica nanocomposite. Chem Mater 12:3397–3401

35. Han S, Kim M, Hyeon T (2003) Direct fabrication of mesoporous carbons using in-situ polymerized silica gel networks as a template. Carbon 41:1525–1532

36. Li HQ, Liu R, Zhao D, Xia Y (2007) Electrochemical properties of an ordered mesoporous carbon prepared by direct tri-constituent co-assembly. Carbon 45:2628–2635

37. Zhuang X, Qian X, Lu J, Wan Y (2010) An alternative method to remove PEO-PPO-PEO template in organic-inorganic mesoporous nanocomposites by sulfuric acid extraction. ApplSurf Sci 256:5343–5348

38. Yoon S, Oh S, Lee C, Ryu J (2011) Pore structure tuning of mesoporous carbon prepared by direct templating method for application to high rate supercapacitor electrodes. J Electroanal Chem 650:187–195

39. Jiang C, Zhou K, Zhong X, Zhong H (2014) A simple organic-inorganic co-assembling route to pore-expanded ordered mesoporous carbons with 2-D hexagonal mesostructure. Powder Technol 259:74–80

40. Prabhu A, Shoaibi A, Srinivasakannan C (2014) Synthesis and characterization of mesoporous carbon by simple one-pot method. Mater Lett 136:81–84

41. Deng Y, Yu T, Wan Y, Shi Y, Meng Y, Gu D, Zhang L, Huang Y, Liu C, Wu X, Zhao D (2007) Ordered mesoporous silicas and carbons with large accessible pores templated from amphiphilic diblock copolymer poly(ethylene oxide)-b-polystyrene. J Am Chem Soc 129:1690–1697

42. Jaroniec M, Gorka J, Choma J, Zawislak A (2009) Synthesis and properties of mesoporous carbons with high loadings of inorganic species. Carbon 47:3034–3040

43. Liu R, Shi Y, Wan Y, Meng Y, Zhang F, Gu D, Chen Z, Tu B, Zhao D (2006) Triconstituent coassembly to ordered mesostructured polymer-silica and carbon silica nanocomposites and large-pore mesoporous carbons with high surface areas. J AmChem Soc 128:11652–11662

44. Sterk L, Gorka J, Vinu A, Jaroniec M (2012) Soft-templating synthesis of ordered mesoporous carbons in the presence of tetraethyl orthosilicate and silver salt. Microporous Mesoporous Mater 156:121–126

45. Su F, Zeng J, Bao X, Yu Y, Lee J, Zhao X (2005) Preparation and characterization of highly ordered graphitic mesoporous carbon as a Pt catalyst support for direct methanol fuel cells. Chem Mater 17:3960–3967